Optics and Photonics Journal, 2023, 13, 47-61
https://www.scirp.org/journal/opj
ISSN Online: 2160-889X
ISSN Print: 2160-8881

Propagation of Gaussian Schell-Model Array Beams through a Jet Engine Exhaust

Huguang Li, Jianyang Zhou*

College of Science, University of Shanghai for Science and Technology, Shanghai, China
Email: *jyzhou@usst.edu.cn

How to cite this paper: Li, H.G. and Zhou, J.Y. (2023) Propagation of Gaussian Schell-Model Array Beams through a Jet Engine Exhaust. *Optics and Photonics Journal*, **13**, 47-61.
https://doi.org/10.4236/opj.2023.133004

Received: February 18, 2023
Accepted: March 27, 2023
Published: March 30, 2023

Abstract

Here a Gaussian Shell Model Array (GSMA) beam is used to investigate the propagation characteristics in the jet engine exhaust region. It has great significance to improve various optical systems for wide application in trapping cold atoms, creating gratings, and atmospheric optical communication. We calculate analytical formulas for the spectral density (SD) and the propagation factors M_x^2 and M_y^2 of a GSMA beam. The influence of inner scale of turbulence in the jet engine exhaust region on its power spectrum has been also analyzed. According to these results, the influence of turbulence in a jet engine exhaust on a GSMA beam has been reduced by changing the parameters of light source and turbulence. For example, it is an excellent tool for mitigation of the jet engine exhaust-induced anisotropy of turbulence to increase the source coherence length, the root-mean-squared (rms) beam width, the wavelength or reduce the outer scale of turbulence.

Keywords

Gaussian Schell Model Array Beams, Jet Engine Exhaust, Spectral Density, Propagation Factors

1. Introduction

In the past investigation, the Gaussian Schell model beams (GSM) have been used to investigate propagation characteristics in turbulence [1]. But in some applications, GSM beam cannot meet the requirements for optical communication. So array beams have been proposed to replace the Gaussian beam in some fields [2]. Compared with the GSM beam, spatially periodic arrays of beams are superior in lidar, laser weapons, capturing cold atoms, making gratings, photonic crystal engineering, and sorting microscopic particles [3] [4]. Based on the sufficient conditions of constructing special correlation function proposed by Gori, Mei proposed the Gaussian Shell model array of beams (GSMA) [5] [6]. Compared with other deterministic array beams, the GSMA beam, which has arbitrary intensity distribution in the initial plane and exhibits optical lattice average intensity patterns in far field, has been studied. These features are important for some applications, such as optical trapping, material processing, and atmospheric optical communications [7] [8].

The propagation characteristics of laser in the atmosphere have been extensively studied [9]-[19]. How to reduce the influence of atmospheric turbulence on laser propagation is also a hotspot in current studies [20] [21]. In classical turbulence models, the power spectrum carries isotropic and uniform statistics. The Kolmogorov model has been always used to characterize turbulence [22]. But in many cases, atmospheric turbulence does not always follow the Kolmogorov model. In previous studies, the existence of turbulent anisotropy in a variety of situations has been demonstrated [23] [24] [25] [26]. Therefore, it has great value to investigate the beam propagation in anisotropic turbulence.

On the other hand, airborne laser systems have been of great interest in recent years due to their potential in aircraft communications and security [27]-[32]. The onboard laser of aircraft faces extremely complex external challenges, and the main one is the plume in the jet area of the aircraft. In previous studies, we can conclude that the power spectrum of a jet plume is anisotropic, and it is related to the structure of aircraft jet system [27]. When the beams pass through the jet engine exhaust area, diffusion occurs in two orthogonal directions, transverse to the optical axis, due to effect of the system on the beams. According to Ref. [33], even over a small distance, the effect of anisotropy can be substantial for GSM beams. Compared with GSM beams, the GSMA beams were better in optical communication. However, to our knowledge, there have been no reports about the GSMA beams in the turbulence of a jet engine exhaust region.

In this work, we have investigated the propagation of the GSMA beams in the turbulence of a jet engine exhaust region. We have not only studied the transmission properties, but also proposed how to reduce the influence of the plume region on the beam transmission. The extended Huygens-Fresnel principle [34] and winger distribution function have been used to obtain the analytical formula [35] for the spectral density (SD) and propagation factors. The influences of the parameters of beams and turbulence on the SD and propagation factors have been studied.

2. Propagation of GSMA Beams across a Jet Engine Exhaust

Consider a GSMA beam located in the $z=0$ plane and radiating a beam-like optical field propagating along z-direction, in a jet engine exhaust. The cross-spectral density (CSD) function of a GSMA beam in the source plane has been expressed by two-dimensional position vectors $\boldsymbol{\rho}_1'=(x_1', y_1')$ and $\boldsymbol{\rho}_2'=(x_2', y_2')$. It has been given as:

$$W(\boldsymbol{\rho}_1',\boldsymbol{\rho}_2',\omega)=\exp\left(-\frac{x_1'^2+x_2'^2}{4\sigma}\right)\exp\left(-\frac{y_1'^2+y_2'^2}{4\sigma}\right)\times\frac{1}{NM}$$
$$\times\exp\left(-\left(\frac{x_1'-x_2'}{2\delta_x}\right)^2\right)\times\sum_{n=-(N-1)/2}^{(N-1)/2}\cos\left(\frac{2\pi nR_x\left(x_1'-x_2'\right)}{\delta_x}\right)$$
$$\times\exp\left(-\left(\frac{y_1'-y_2'}{2\delta_y}\right)^2\right)\times\sum_{m=-(M-1)/2}^{(M-1)/2}\cos\left(\frac{2\pi mR_y\left(y_1'-y_2'\right)}{\delta_y}\right). \quad (1)$$

where σ is the incident root-mean-squared width. δ_x and δ_y are the coherence length along x and y directions. M and N are parameters that can control array dimension. R_x R_y control the sub-beams space. ω is the angular frequency, we ignore the beams dependence on ω to facilitate calculation.

When beams propagate in the turbulence, the extended Huygens-Fresnel principle and paraxial approximation have been used to calculate the CSD function in the positive direction of the z-axis.

$$W(\boldsymbol{\rho}_1,\boldsymbol{\rho}_2,z)=\frac{1}{\lambda^2z^2}\int_{-\infty}^{\infty}\int_{-\infty}^{\infty}W^{(0)}(\boldsymbol{\rho}_1',\boldsymbol{\rho}_2')\exp\left[-\frac{ik}{2z}(\boldsymbol{\rho}_1-\boldsymbol{\rho}_1')^2+\frac{ik}{2z}(\boldsymbol{\rho}_2-\boldsymbol{\rho}_2')^2\right]$$
$$\times\left\langle\exp\left[\psi^*(\boldsymbol{\rho}_1,\boldsymbol{\rho}_1',z)+\psi(\boldsymbol{\rho}_2,\boldsymbol{\rho}_2',z)\right]\right\rangle\mathrm{d}^2\boldsymbol{\rho}_1'\mathrm{d}^2\boldsymbol{\rho}_2'. \quad (2)$$

where $\boldsymbol{\rho}_1=(x_1,y_1)$ and $\boldsymbol{\rho}_2=(x_2,y_2)$ are two points in the transverse plane when $z>0$. $k=2\pi/\lambda$ is wave number, λ is the wavelength of light.
$\psi(\boldsymbol{\rho},\boldsymbol{\rho}',z)$ stands for the complex phase perturbation which is caused by random media. The asterisk represents complex conjugate. Here angle bracket implies mean ensemble of turbulence (see **Figure 1**).

According to Ref. [33], the content in angle bracket is expressed by follow:

$$\left\langle\exp\left[\psi^*(\boldsymbol{\rho}_1,\boldsymbol{\rho}_1',z)+\psi(\boldsymbol{\rho}_2,\boldsymbol{\rho}_2',z)\right]\right\rangle$$
$$=\exp\left\{-2\pi k^2z\int_0^1\mathrm{d}t\int\mathrm{d}^2\boldsymbol{\kappa}\Phi_n(\boldsymbol{\kappa})\left[1-\exp\left(t\boldsymbol{\rho}_d\cdot\boldsymbol{\kappa}+(1-t)\boldsymbol{r}_d\cdot\boldsymbol{\kappa}\right)\right]\right\}. \quad (3)$$

In this function, we consider the anisotropic power spectrum of the jet engine exhaust, according to Ref. [27]:

$$\Phi_n(\kappa)=0.033C_n^2\times\left\{\frac{\left(L_{0x}L_{0y}\right)^{11/6}}{\left[1+\left(\kappa_xL_{0x}\right)+\left(\kappa_yL_{0y}\right)\right]^{11/6}}\exp\left(-\frac{\kappa_x^2}{\kappa_{mx}^2}-\frac{\kappa_y^2}{\kappa_{my}^2}\right)\right.$$
$$\left.+Q\left[\left(\frac{2\pi}{L_s}\right)^2+\kappa^2\right]^{-11/6}\exp\left(-\kappa^2/\kappa_m^2\right)\right\}. \quad (4)$$

where $\boldsymbol{\rho}_d=\boldsymbol{\rho}_1-\boldsymbol{\rho}_2$ and $\boldsymbol{\rho}_d=\boldsymbol{\rho}_1'-\boldsymbol{\rho}_2'$. $\boldsymbol{\kappa}=(\kappa_x,\kappa_y)$ is the two-dimensional spatial frequency vector. L_{0x} and L_{0y} are outer scales, l_{0x} and l_{0y} are inner scales in x and y directions. $\kappa_m=c(\alpha)/l_0$, $\kappa_{mx}=c(\alpha)/l_{0x}$ and $\kappa_{my}=c(\alpha)/l_{0y}$. Here $l_0=\sqrt{l_{0x}^2+l_{0y}^2}$.

In Equation (5) we define the $c(\alpha)$:

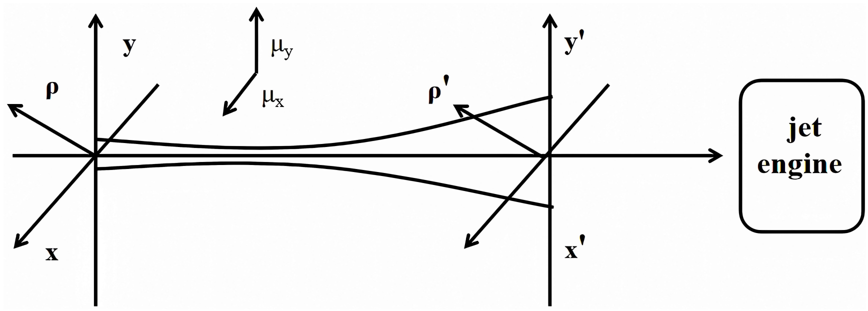

Figure 1. Schematic diagram for propagation of a GSMA beam through a jet engine exhaust.

$$c(\alpha)=\left[\frac{2\pi\Gamma(5-\alpha/2)A(\alpha)}{2}\right]^{\frac{1}{\alpha-5}}. \tag{5}$$

where the Γ is Gamma Function. The $A(\alpha)$ can be expressed:

$$A(\alpha)=\frac{1}{4\pi^2}\Gamma(\alpha-1)\cos\left(\frac{\alpha\pi}{2}\right), 3<\alpha<4. \tag{6}$$

We can obtain an analytical expression of the power spectrum and express it as the sum of A plus B. In this place, we set α equal to 11/3:

$$\left\langle \exp\left[\psi^*(\rho_1',\rho_1,z)+\psi(\rho_2',\rho_2,z)\right]\right\rangle = A+B, \tag{7}$$

$$A=\exp\left\{-\frac{\pi^2k^2zT_A\left(x_d^2+x_dx_d'+x_d'^2\right)}{3\mu_x^2}\right\}\exp\left\{-\frac{\pi^2k^2zT_A\left(y_d^2+y_dy_d'+y_d^2\right)}{3\mu_y^2}\right\}, \tag{8}$$

$$B=\exp\left[-\frac{1}{3}\pi^2k^2zT_B\left(x_d^2+x_dx_d'+x_d'^2\right)\right]\exp\left[-\frac{1}{3}\pi^2k^2zT_B\left(y_d^2+y_dy_d'+y_d'^2\right)\right], \tag{9}$$

where the T_A and T_B have been expressed as:

$$\begin{aligned} T_A &= \frac{1}{\mu_x\mu_y}\int_0^\infty \kappa'^3\Phi_{n1}'(\kappa')\,\mathrm{d}\kappa' \\ &= 0.033C_n^2\left(\mu_x\mu_y\right)^{\frac{5}{6}}\left[\frac{\left(5+\frac{6}{\kappa_m^2L_0^2}\right)\exp\left(\frac{1}{\kappa_m^2L_0^2}\right)\Gamma\left(\frac{1}{6},\frac{1}{\kappa_m^2L_0^2}\right)}{10\left(\frac{1}{\kappa_m^2}\right)^{\frac{1}{6}}}-\frac{3}{5}\left(\frac{1}{L_0^2}\right)^{\frac{1}{6}}\right], \end{aligned} \tag{10}$$

$$\begin{aligned} T_B &= \int_0^\infty \kappa^3\Phi_{n2}(\kappa)\,\mathrm{d}\kappa \\ &= 0.033C_n^2Q\left[\frac{\left(5+\frac{24\pi^2}{\kappa_m^2L_s^2}\right)\exp\left(\frac{4\pi^2}{\kappa_m^2L_s^2}\right)\Gamma\left(\frac{1}{6},\frac{4\pi^2}{\kappa_m^2L_s^2}\right)}{10\left(\frac{1}{\kappa_m^2}\right)^{\frac{1}{6}}}-\frac{3}{5}\left(\frac{4\pi^2}{L_s^2}\right)^{\frac{1}{6}}\right]. \end{aligned} \tag{11}$$

By applying (2) (7) and (8). Then, we orthogonally separate A into x and y. We will get the CSD function in the x direction:

$$W_{xA}\left(x_1,x_2,z\right)=\frac{k\sigma}{2\sqrt{2}N\sqrt{\Delta_{xA}\left(z\right)}}\exp\left(-\frac{x_d}{R_{xA}\left(z\right)}\right)\times\sum_{n=-(N-1)/2}^{(N-1)/2}\left[\exp\left(\frac{\gamma_{xA+}^2\left(z\right)}{4\Delta_{xA}\left(z\right)}\right)+\exp\left(\frac{\gamma_{xA-}^2\left(z\right)}{4\Delta_{xA}\left(z\right)}\right)\right],\tag{12}$$

here

$$\frac{1}{R_{xA}\left(z\right)}=\frac{k^2\sigma^2}{2z^2}+\frac{\pi^2k^2zT_A}{3\mu_x^2},\tag{13}$$

$$\Delta_{xA}(z)=\frac{1}{8\sigma^2}+\frac{1}{2\delta_x^2}+\frac{1}{R_{xA}\left(z\right)},\tag{14}$$

$$\gamma_{xA\pm}\left(z\right)=\left(\frac{\pi^2k^2zT_A}{3\mu_x^2}-\frac{k^2\sigma^2}{z^2}\right)x_d+\frac{ikx_s}{z}\pm\frac{i2\pi nR_x}{\delta_x}.\tag{15}$$

It is the same in both orthogonal directions. W_A can be expressed by:

$$W_A=W_{xA}W_{yA}.\tag{16}$$

Substituting Equation (9) into Equation (2), we will get the CSD function of B part:

$$W_B\left(\rho_1,\rho_2,z\right)=\frac{k^2\sigma^2}{8NMz^2\sqrt{\Delta_{xB}\left(z\right)\Delta_{yB}\left(z\right)}}\exp\left(-\frac{x_d^2+y_d^2}{R_B\left(z\right)}\right)\times\sum_{n=-(N-1)/2}^{(N-1)/2}\left[\exp\left(\frac{\gamma_{xB+}^2\left(z\right)}{4\Delta_{xB}\left(z\right)}\right)+\exp\left(\frac{\gamma_{xB-}^2\left(z\right)}{4\Delta_{xB}\left(z\right)}\right)\right]\times\sum_{m=-(M-1)/2}^{(M-1)/2}\left[\exp\left(\frac{\gamma_{yB+}^2\left(z\right)}{4\Delta_{yB}\left(z\right)}\right)+\exp\left(\frac{\gamma_{yB-}^2\left(z\right)}{4\Delta_{yB}\left(z\right)}\right)\right].\tag{17}$$

where parameters Δ_{jB}, R_B and γ_{jB} are given by expressions:

$$\frac{1}{R_B\left(z\right)}=\frac{k^2\sigma^2}{2z^2}+\frac{\pi^2k^2zT_B}{3},\tag{18}$$

$$\Delta_{jB}\left(z\right)=\frac{1}{8\sigma^2}+\frac{1}{2\delta_j^2}+\frac{1}{R_B\left(z\right)},\tag{19}$$

$$\gamma_{jB\pm}\left(z\right)=\left(\frac{\pi^2k^2zT_B}{3}-\frac{k^2\sigma^2}{z^2}\right)j_d+\frac{ikj}{z}\pm\frac{i2\pi mR_j}{\delta_j}\left(j=x,y\right).\tag{20}$$

For scalar random beams the spectral density (SD) and the spectral degree of coherent (DOC) can be expressed by the forms of follow:

$$S\left(\rho,\omega\right)=W\left(\rho,\rho,z\right)=W_A\left(\rho,\rho,z\right)+W_B\left(\rho,\rho,z\right),\tag{21}$$

$$\mu\left(\rho_1,\rho_2,z\right)=\frac{W\left(\rho_1,\rho_2,z\right)}{\sqrt{S\left(\rho_1,z\right)S\left(\rho_2,z\right)}}=\frac{W_A\left(\rho_1,\rho_2,z\right)+W_B\left(\rho_1,\rho_2,z\right)}{\sqrt{\left[W_A\left(\rho_1,\rho_1,z\right)+W_B\left(\rho_1,\rho_1,z\right)\right]\left[W_A\left(\rho_2,\rho_2,z\right)+W_B\left(\rho_2,\rho_2,z\right)\right]}}.\tag{22}$$

For GSMA beams, the propagation factors in the *x*, *y* directions can be used to represent transmission quality, which are defined as

$$M_x^2(z) = 2k\left(\left\langle x^2\right\rangle_z \left\langle \theta_x^2\right\rangle_z - \left\langle x\cdot\theta_x\right\rangle_z^2\right)^{1/2}, \tag{23}$$

$$M_y^2(z) = 2k\left(\left\langle y^2\right\rangle_z \left\langle \theta_y^2\right\rangle_z - \left\langle y\cdot\theta_y\right\rangle_z^2\right)^{1/2}. \tag{24}$$

Here, $\left\langle x^2\right\rangle_z$, $\left\langle \theta_x^2\right\rangle_z$, $\left\langle x\cdot\theta_x\right\rangle_z$, $\left\langle \theta_y^2\right\rangle_z$ and $\left\langle y\cdot\theta_y\right\rangle_y$ are the second-order statistics of the GSMA beam transmit to the *z*-plane. They have been defined as follows:

$$\left\langle x^{n_1} y^{n_2} \theta_x^{m_1} \theta_y^{m_2}\right\rangle_z = \frac{1}{P}\iiiint_{-\infty}^{\infty} x^{n_1} y^{n_2} \theta_x^{m_1} \theta_y^{m_2} h\left\langle x, y, \theta_x, \theta_y, z\right\rangle \mathrm{d}x\mathrm{d}y\mathrm{d}\theta_x\mathrm{d}\theta_y, \tag{25}$$

$$P = \iiiint_{-\infty}^{\infty} h\left\langle x, y, \theta_x, \theta_y, z\right\rangle \mathrm{d}x\mathrm{d}y\mathrm{d}\theta_x\mathrm{d}\theta_y. \tag{26}$$

where, $h\left\langle x, y, \theta_x, \theta_y, z\right\rangle$ is the Wigner distribution function, which can be represented by the two-dimensional Fourier transform of the cross spectral density:

$$h\left\langle x, y, \theta_x, \theta_y, z\right\rangle = \left(\frac{k}{2\pi}\right)^2 \iint_{-\infty}^{\infty} W(\rho_1, \rho_2, z)\exp\left(-ikx_d\theta_x - iky_d\theta_y\right)\mathrm{d}x_d\mathrm{d}y_d. \tag{27}$$

After complex calculation, we can get:

$$\begin{aligned} M_x^2(z) = \Bigg[&\left(4\sigma^2 + 16\pi^2 T_A z^3/3\mu_x^2\right)\left(\frac{1}{4\sigma^2} + \frac{1}{\delta_x^2} + \frac{1}{N-1}\sum_{n=-(N-1)/2}^{(N-1)/2}\frac{4\pi^2 n^2 R_x^2}{\delta_x^2}\right) \\ &+ 16k^2\sigma^2\pi^2 T_A z/3\mu_x^2 + 8k^2\pi^4 T_A^2 z/9\mu_x^4\Bigg]^{1/2}, \end{aligned} \tag{28}$$

$$\begin{aligned} M_y^2(z) = \Bigg[&\left(4\sigma^2 + 16T_A z^3/3\mu_y\right)\left(\frac{1}{4\sigma^2} + \frac{1}{\delta_y^2} + \frac{1}{M-1}\sum_{m=-(M-1)/2}^{(M-1)/2}\frac{4\pi^2 m^2 R_y^2}{\delta_y^2}\right) \\ &+ 16k^2\sigma^2 T_A z/3\mu_y + 8k^2 T_A^2 z/9\mu_y^2\Bigg]^{1/2}. \end{aligned} \tag{29}$$

Next, we will analyze the analytical formulas.

3. Numerical Computation and Analysis

In this part, the analytical formulas (21), (28) and (29) which obtained in the second part have been used to simulate the SD and propagation factors evolution of a GSMA beam when it passes through the engine exhaust region. The parameters are set to $\sigma_0 = 1\ \mathrm{mm}$, $\lambda = 632.8\ \mathrm{nm}$, $C_n^2 = 1.6\times10^{-9}\ \mathrm{m}^{-2/3}$, $L_0 = 0.5\ \mathrm{m}$, $L_s = 1\ \mathrm{mm}$, $\mu_x = 0.7$, $\mu_y = 1.4$, $\delta_x = \delta_y = 0.5\ \mathrm{mm}$ and $Q = 6$. Except as specified, the above parameters remain unchanged.

In Figure 2, we plotted the exponential of the anisotropy power spectrum of turbulence refractive index with changes in *x* and *y* directions. We can see from Figure 2 that according to Equation (4) in the second part, when the turbulence internal scale value we selected is greater than $l_0 = 1\ \mathrm{mm}$, the power spectrum Φ_n varies significantly in the high spatial frequency region between 10^3 and 10^4.

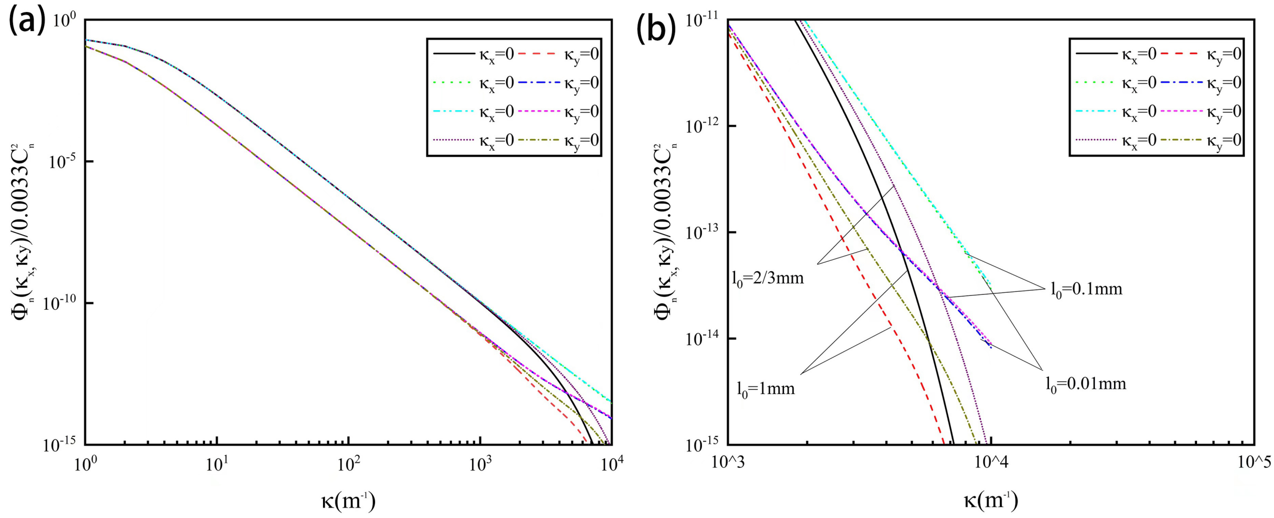

Figure 2. Variation of the anisotropic power spectrum of refractive index fluctuations along the *x* and *y* directions of the jet exhaust region according to Equation (4).

When the inner scale of the turbulence is $l_0 = 0.1\text{ mm}$ and $l_0 = 0.01\text{ mm}$, the power spectrum Φ_n coincide in the *x* and *y* directions without obvious change. The obtained data can more intuitive, when the inner scale of the turbulence is determined as $l_0 = 2/3\text{ mm}$.

According to Equation (12) and Equation (16), we can find that W_B has no anisotropic terms compared with W_A. Therefore, W_A has contributed greatly to defining the anisotropic characteristics of SD, so the evolution of W_A has been focused. Figure 3 shows the evolution of SD of GSMA beam over a certain propagation distance at three different source coherence widths $\delta_x = \delta_y = 1\text{ mm}$, $\delta_x = \delta_y = 0.5\text{ mm}$ and $\delta_x = \delta_y = 0.1\text{ mm}$. Because of the actual length of the jet exhaust zone, the range selected here is much smaller than that used for transport in atmospheric turbulence. As can be seen from the pictures (d) (e) (f) or (g) (h) (i), with the increase of propagation distance, the beam intensity profile gradually splits, forming array distribution. In the propagation process, the transverse diffraction effect of turbulence increases gradually and destroys the array distribution gradually. Compared with (a) (d) (g), (b) (e) (h) or (c) (f) (i), we can find that for the same propagation distance under different coherent length, the GSMA beam become more resistant to turbulence due to reduction of coherence length. For almost coherent source, the influence of turbulence is much bigger. This means that we can effectively resist the transverse diffraction effect of turbulence by reducing the coherence length of the source field.

In Figure 4, supplementary explanation has been made for parameters to affect spectral density. In Figure 4, the coherence length of source selected by any image is $\delta_x = \delta_y = 0.5\text{ m}$. As can be seen from Figure 4, R_x, R_y can adjust the spacing between sub-beams and *N*, *M* can adjust the number of sub-beams in *x* and *y* directions respectively. By contrast with (a) (d) (g), (b) (e) (h), (c) (f) (i), when $R_x = 1$ in the *x* direction, the connection between sub-beams becomes difficult to distinguish. When $R_x = 2$, the independence of sub beam is enhanced.

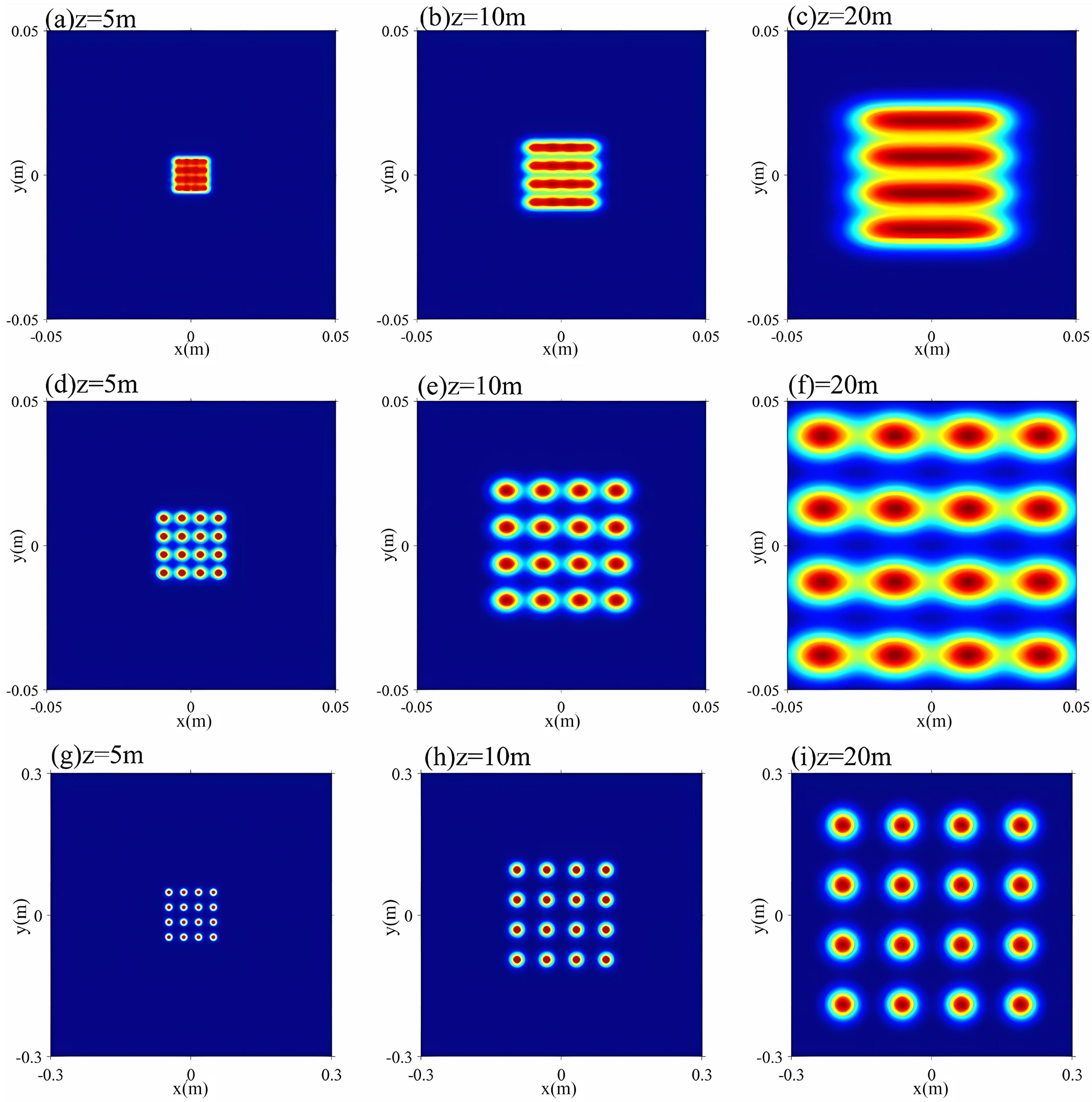

Figure 3. In the jet engine exhaust area, the evolution of the SD of the GSMA beams with the propagation distance under different δ_x and δ_y conditions: (a)-(c) $\delta_x = \delta_y = 1\ \text{mm}$, (d)-(f) $\delta_x = \delta_y = 0.5\ \text{mm}$, (g)-(i) $\delta_x = \delta_y = 0.1\ \text{mm}$.

Therefore, increasing the space between sub-beams can effectively increase the resistance of beams to turbulence.

It can be seen from past investigation that the GSMA beam was more resistant to turbulence than the GSM beam. According to Figure 5, the GSMA beam is gentler than the GSM beam curve in the x and y directions, which means that within a given propagation range, under the same beam parameters, the transmission quality of the GSMA beam is much better than the GSM beam in the turbulence of a jet engine exhaust region.

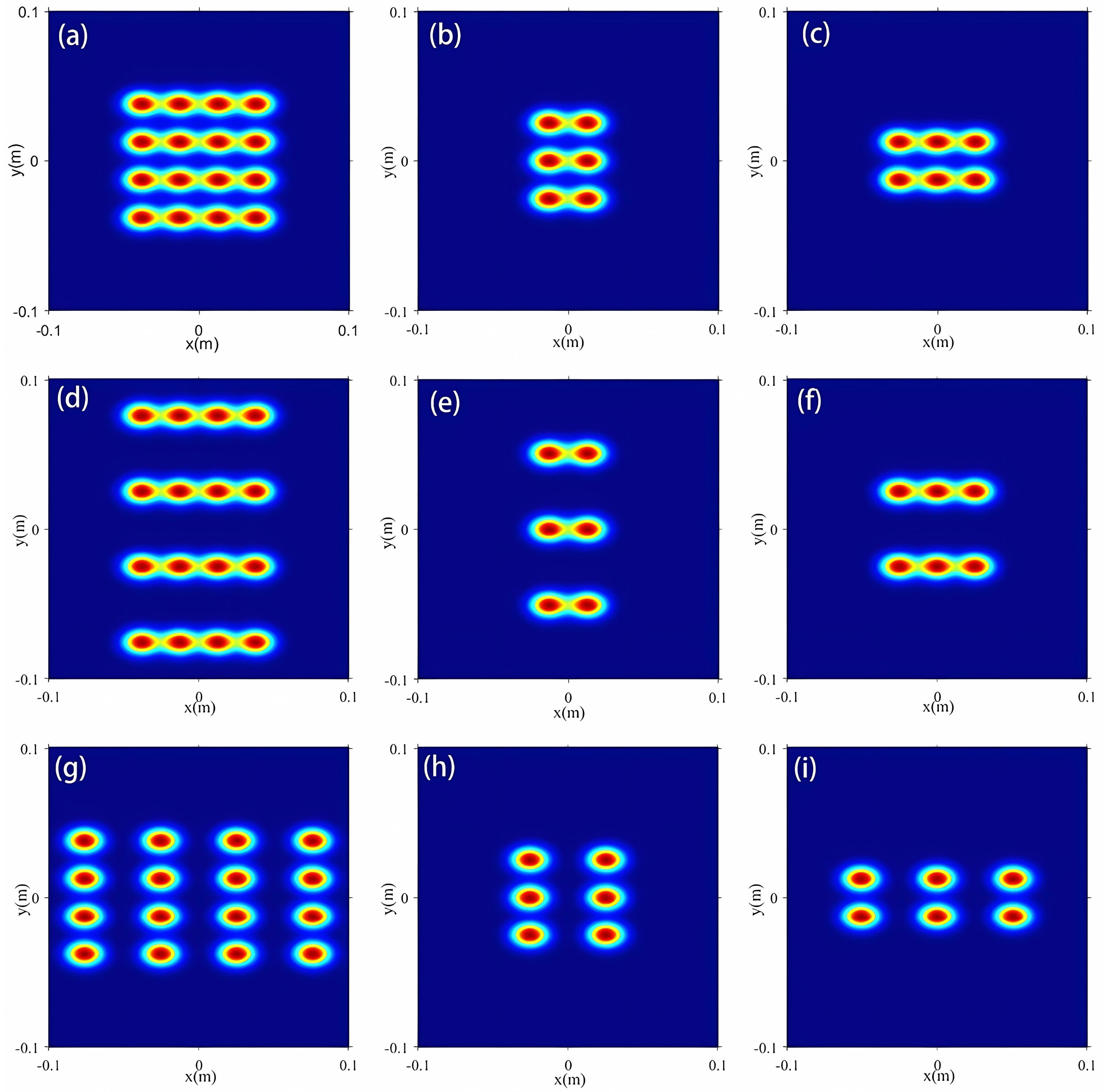

Figure 4. In the jet engine exhaust area, selecting different initial parameters M, N, R_x, R_y, S the distribution of the spectral density S of the GSMA beam when it has transmitted to the distance $z = 20\text{ m}$.

Next, the parameters of the beam and the turbulence have been changed within a reasonable range to observe the influence between the GSMA beam and turbulence on the propagation factors. Although the influence of turbulence on the light source is anisotropic, the changing trend of the influence in the x direction and the y direction is the same. Since the turbulence in the x direction has a large influence on the beam, we have analyzed the transmission quality in the x direction.

Firstly, consider the influence of light source parameter changes on the GSMA beam in the exhaust area of the jet engine, such as the number of sub-beams N,

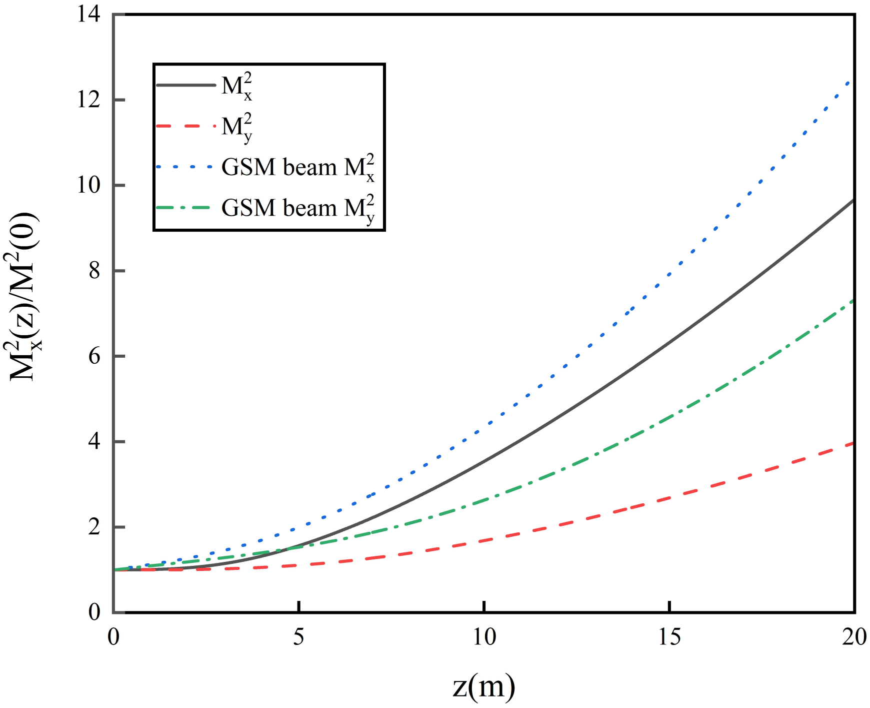

Figure 5. Graph of normalized propagation factors versus propagation distance in the jet engine exhaust region under the same parameters for the GSM beam and the GSMA beam.

the sub-beam spacing R_x, the coherence length δ_x, the wavelength λ, the beam width σ for the normalized M_x^2 influences. Figure 6 shows the variation curve of the propagation factor M_x^2 with the propagation distance under different values of δ_x, N and R_x. It can be seen from (a), (b), (c), (d) that in a small coherence length, the influence of the R_x and N changes on the propagation factors are almost unchanged. But as the coherence length increases, the slope of curve goes up and the impaction by R_x and N becomes apparent. In either picture, the sub-beam spacing R_x and the array dimension N have a great influence on the propagation factor M_x^2. This means that we can reduce the coherence length δ_x, the sub-beam spacing R_x and the array dimension N to increase the resistance of the beam on turbulence.

The effect of wavelength λ and beam width σ on the propagation factor can be seen from Figure 7. When the wavelength and beam width increase, the propagation factor decreases. Therefore, the propagation factor can be reduced by increasing the wavelength or the beam width σ.

Earlier we discussed the effect of the initial parameters of the beam on the transmission quality. Next, we discuss the effect of turbulence parameters on the transmission quality. Figure 8 shows the variation of the propagation factor M_x^2 corresponding to different refractive index structure constants C_n^2, different turbulent outer scale L_0 and different turbulent inner scale l_0. It is shown that the refractive index structure constants C_n^2 can affect the intensity of turbulence. For less intense turbulence, the curve is much flatter, the quality of

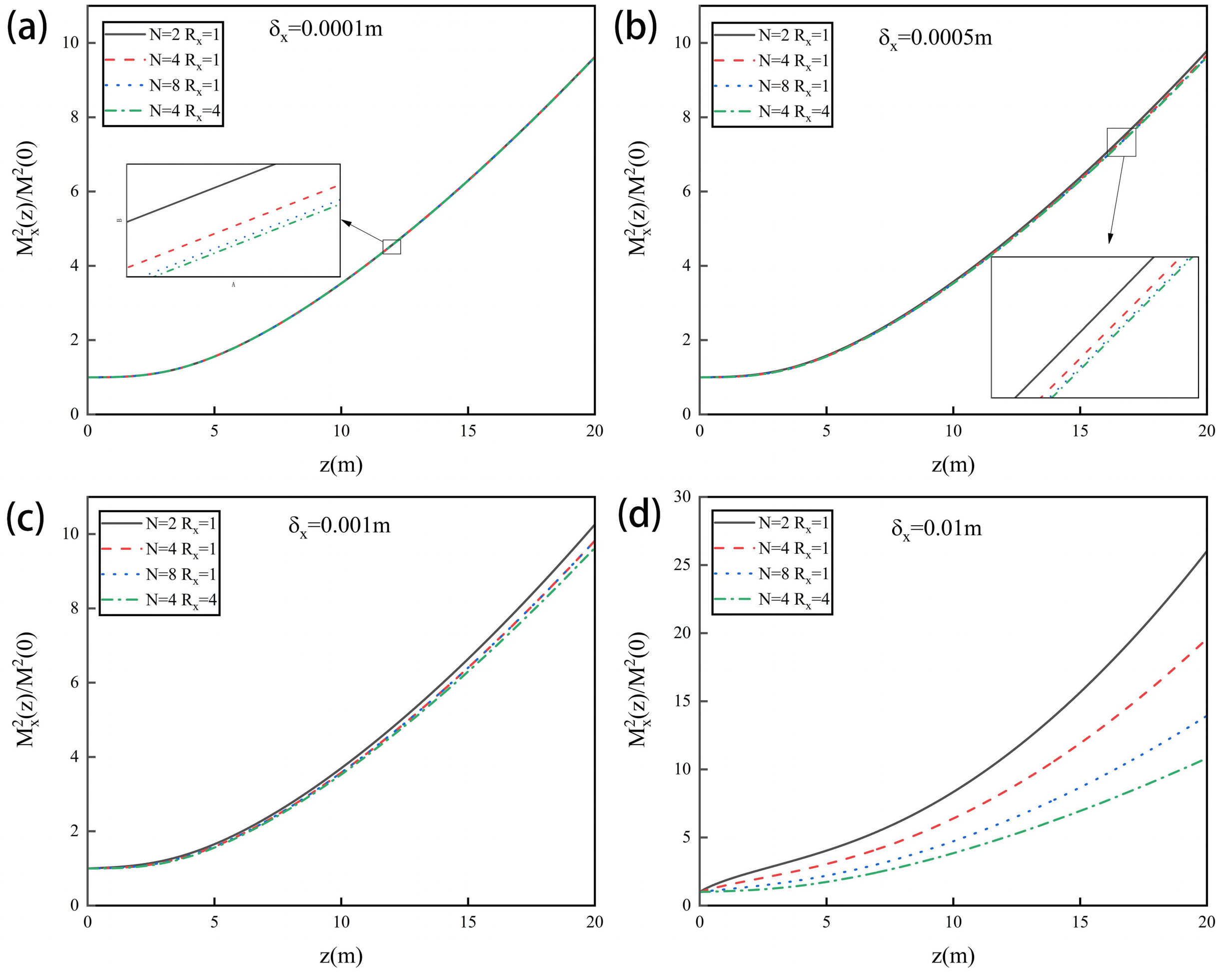

Figure 6. The curve of the normalized M_x^2 factor of the GSMA beam as a function of the transmission distance when the coherence length δ is selected with different values. (a) $\delta_x = 0.0001\ \text{m}$; (b) $\delta_x = 0.0005\ \text{m}$; (c) $\delta_x = 0.001\ \text{m}$; (d) $\delta_x = 0.01\ \text{m}$.

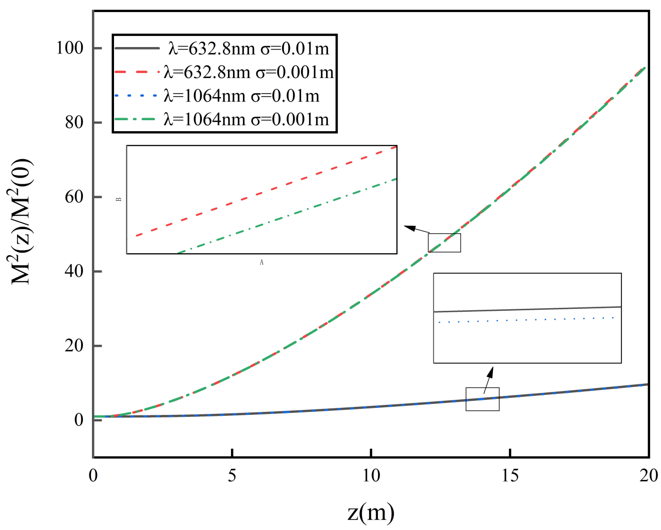

Figure 7. The curve of the normalization factor M_x^2 of the GSMA beam as a function of the transmission distance when the wavelength λ and beam width σ are selected with different values.

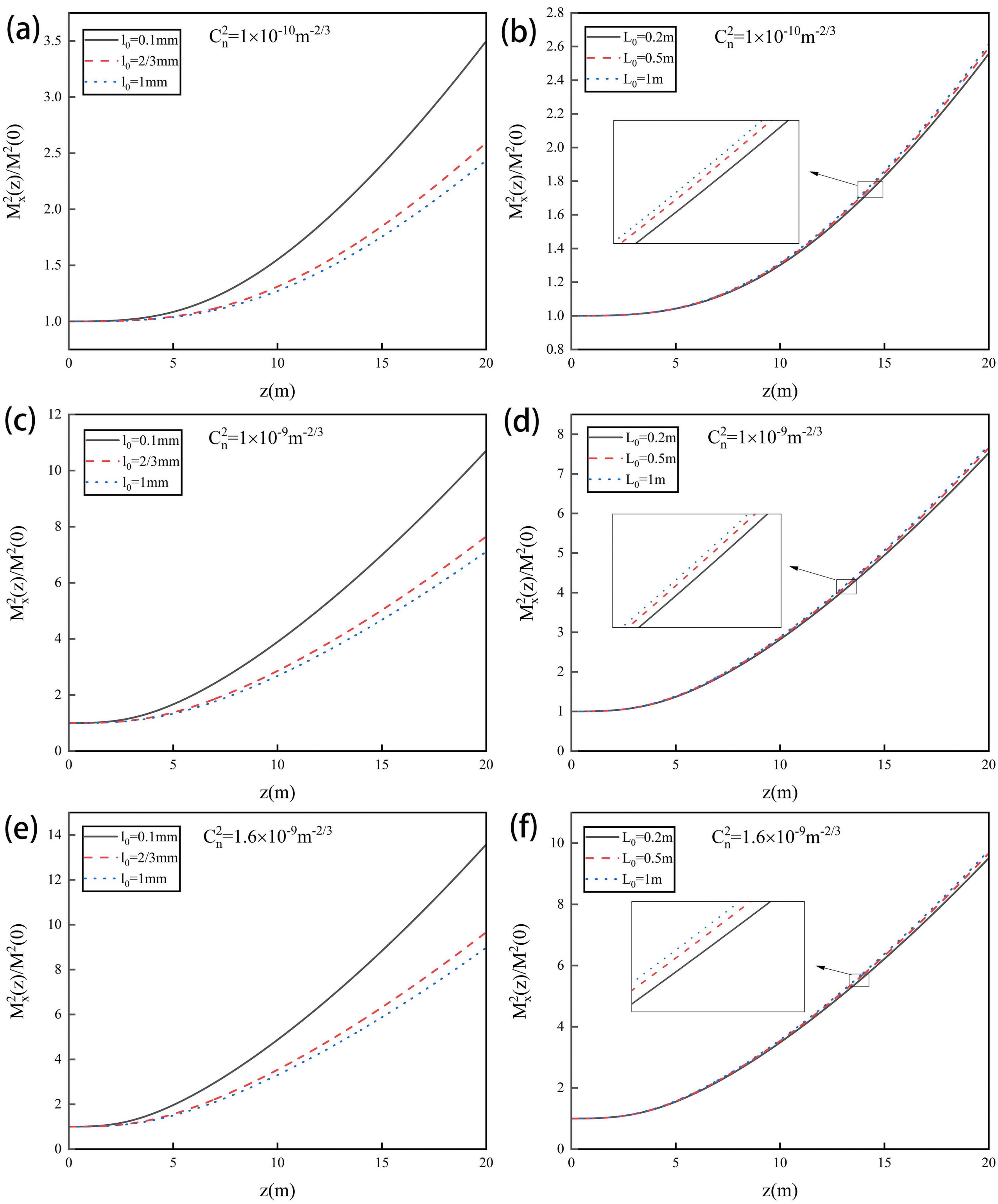

Figure 8. With different generalized refractive index structure parameters, the normalization factor M_x^2 of the GSMA beam varies with the transmission distance, where (a) (b) $C_n^2 = 1\times10^{-10}\ \mathrm{m}^{-2/3}$; (c) (d) $C_n^2 = 1\times10^{-9}\ \mathrm{m}^{-2/3}$; (e) (f) $C_n^2 = 1.6\times10^{-9}\ \mathrm{m}^{-2/3}$.

transmission is much better. Meanwhile, according to Ref. [27], we have selected the various constants of turbulence within a suitable range. When we change the inner scale l_0, the size of the outer scale L_0 is fixed to $L_0 = 0.5\text{ m}$. When we change the outer scale L_0, the size of the inner scale l_0 is fixed as $l_0 = 2/3\text{ m}$. When the refractive index structure constant takes a fixed value, reducing the inner scale l_0 and increasing the outer scale L_0 can both increase the resistance of the beam to turbulence. Meanwhile, the normalized propagation factor M_x^2 is not sensitive to changes in the outer scale L_0, especially in the case of strong turbulence. Therefore, increase the inner dimension l_0 is better for beam to propagate than reduce the outer dimension L_0.

4. Conclusion

Based on the Huygens-Fresnel principle and the Winger distribution function, we calculated the analytical expressions of the spectral density and propagation factors of the GSMA beams. When the GSMA beams propagate in the exhaust region of a jet engine (which can be approximated as an anisotropic non-Kolmogorov turbulent flow with extremely high turbulence intensity), the beams spread along two mutually orthogonal directions, transverse to the optical axis. And we use the propagation factors to represent the quality of the GSMA beam. We can increase the array dimension, the relative distance between the sub-beams, the beam width and the wavelength, or reduce the coherence length to improve the resistance of beam to turbulence. In terms of the influence of turbulence parameters on transmission quality, when the inner scale and outer scale have been fixed, the larger refractive index structure constants destroy the beam transmission. We can increase the inner scale or reduce the outer scale to improve the beam transmission. And in the same situation, increasing the inner scale is better for beam transmission than reducing the outer scale.

Conflicts of Interest

The authors declare no conflicts of interest regarding the publication of this paper.

References

[1] Ji, X., Zhang, E. and Lu, B. (2006) Changes in the Spectrum of Gaussian Schell-Model Beams Propagating through Turbulent Atmosphere. *Optics Communications*, **259**, 1-6. https://doi.org/10.1016/j.optcom.2005.08.019

[2] Sahin, S. and Korotkova, O. (2012) Light Sources Generating Far Fields with Tunable Flat Profiles. *Optics Letters*, **37**, 2970-2972. https://doi.org/10.1364/OL.37.002970

[3] Anderson, B.P., Gustavson, T.L. and Kasevich, M.A. (1996) Atom Trapping in Nondissipative Optical Lattices. *Physical Review A*, **53**, R3727-R3730. https://doi.org/10.1103/PhysRevA.53.R3727

[4] MacDonalda, M.P., Neale, S., Paterson, L., Riches, A., Spalding, G.C. and Dholakia, K. (2003) Microfluidic Optical Sorting: Particle Selection in an Optical Lattice. *Nature*, **426**, 421-424. https://doi.org/10.1038/nature02144

[5] Gori, F. and Santarsiero, M. (2007) Devising Genuine Spatial Correlation Functions.

Optics Letters, **32**, 3531-3533. https://doi.org/10.1364/OL.32.003531

[6] Mei, Z., Zhao, D., Korotkova, O. and Mao, Y. (2015) Gaussian Schell-Model Arrays. *Optical Letters*, **40**, 5662-5665. https://doi.org/10.1364/OL.40.005662

[7] Neuman, K.C. and Block, S.M. (2004) Optical Trapping. *Review of Scientific Instruments*, **75**, 2787-809. https://doi.org/10.1063/1.1785844

[8] Mao, Y., Mei, Z. and Gu, J. (2016) Propagation of Gaussian Schell-Model Array Beams in Free Space and Atmospheric Turbulence. *Optics & Laser Technology*, **86**, 14-20. https://doi.org/10.1016/j.optlastec.2016.06.007

[9] Gu, Y.L. and Gbur, G. (2013) Scintillation of Nonuniformly Correlated Beams in Atmospheric Turbulence. *Optics Letters*, **38**, 1395-1397. https://doi.org/10.1364/OL.38.001395

[10] Du, S.C., Yuan, Y.S., Liang, C.H. and Cai, Y.J. (2013) Second-Order Moments of a Multi-Gaussian Schell-Model Beam in a Turbulent Atmosphere. *Optics and Laser Technology*, **50**, 14-19. https://doi.org/10.1016/j.optlastec.2013.01.027

[11] Yuan, Y.S., Liu, X.L., Wang, F., Chen, Y.H., Cai, Y.J., Qu, J. and Eyyuboglu, H.T. (2013) Scintillation Index of a Multi-Gaussian Schell-Model Beam in Turbulent Atmosphere. *Optics Communications*, **305**, 57-65. https://doi.org/10.1016/j.optcom.2013.04.076

[12] Korotkova, O., Avramov-Zamurovic, S., Nelson, C., Malek-Madani, R., Gu, Y. and Gbur, G. (2014) Scintillation Reduction in Multi-Gaussian Schell-Model Beams Propagating in Atmospheric Turbulence. *Proceedings of the SPIE*, **9224**, 92240M. https://doi.org/10.1117/12.2062601

[13] Xu, H.F., Zhang, Z., Qu, J. and Huang, W. (2014) Propagation Factors of Cosine-Gaussian-Correlated Schell-Model Beams in Non-Kolmogorov Turbulence. *Optics Express*, **22**, 22479-22489. https://doi.org/10.1364/OE.22.022479

[14] Chen, R., Liu, L., Zhu, S.J., Wu, G.F., Wang, F. and Cai, Y.J. (2014) Statistical Properties of a Laguerre-Gaussian Schell-Model Beam in Turbulent Atmosphere. *Optics Express*, **22**, 1871-1883. https://doi.org/10.1364/OE.22.001871

[15] Wang, X.Y., Yao, M.W., Qiu, Z.L., Yi, X. and Liu, Z.J. (2015) Evolution Properties of Bessel-Gaussian Schell-Model Beams in Non-Kolmogorov Turbulence. *Optics Express*, **23**, 12508-12523. https://doi.org/10.1364/OE.23.012508

[16] Xu, Y., Li, Y., Dan, Y., Du, Q. and Wang, S. (2016) Propagation Based on Second-Order Moments for Partially Coherent Laguerre-Gaussian Beams through Atmospheric Turbulence. *Journal of Modern Optics*, **63**, 1121-1128. https://doi.org/10.1080/09500340.2015.1128006

[17] Zhou, Y., Yuan, Y.S., Qu, J. and Huang, W. (2016) Propagation Properties of Laguerre-Gaussian Correlated Schell-Model Beam in Non-Kolmogorov Turbulence. *Optics Express*, **24**, 10682-10693. https://doi.org/10.1364/OE.24.010682

[18] Lungu, J., Siwale, L., Kashinga, R.J., Chama, S. and Bereczky, A. (2021) Correlation of Performance, Exhaust Gas Temperature and Speed of a Spark Ignition Engine Using Kiva4. *Journal of Power and Energy Engineering*, **9**, 53-78. https://doi.org/10.4236/jpee.2021.98004

[19] Ighodaro, O., Aburime, E. and Erameh, A. (2022) Off-Design Modelling of a Turbo Jet Engine with Operative Afterburner. *Open Journal of Energy Efficiency*, **11**, 88-107. https://doi.org/10.4236/ojee.2022.113007

[20] Cai, Y. and Zhu, S.-Y. (2004) Ghost Interference with Partially Coherent Radiation. *Optics Letters*, **29**, 2716-2718. https://doi.org/10.1364/OL.29.002716

[21] Zhou, P., Liu, Z.J., Xu, X.J. and Chu, X.X. (2009) Propagation of Coherently Com-

bined Flattened Laser Beam Array in Turbulent Atmosphere. *Optics and Laser Technology*, **41**, 403-407. https://doi.org/10.1016/j.optlastec.2008.08.009

[22] Andrews, L.C. and Phillips, R.L. (2005) Laser Beams Propagation through Random Media, 2nd Edition. SPIE Press, Bellingham, WA. https://doi.org/10.1117/3.626196

[23] Robert, C., Conan, J.M., Michau, V., Renard, J.B., Robert, C. and Dalaudier, F. (2008) Retrieving Parameters of the Anisotropic Refractive Index Fluctuations Spectrum in the Stratosphere from Balloon-Borne Observations of Stellar Scintillation. *Journal of the Optical Society of America A*, **25**, 379-393. https://doi.org/10.1364/JOSAA.25.000379

[24] Otten, L.J., Roggemann, M.C., Al Jones, B., Lane, J. and Black, D.G. (1999) High Bandwidth Atmospheric Turbulence Data Collection Platform. *SPIE PRESS*, **3866**, 23-32. https://doi.org/10.1117/12.371331

[25] Wang, F. and Korotkova, O. (2016) Random Optical Beam Propagation in Anisotropic Turbulence along Horizontal Links. *Optics Express*, **24**, 24422-24434. https://doi.org/10.1364/OE.24.024422

[26] Grechko, G.M., Gurvich, A.S., Kan, V., Kireev, S.V. and Savchenko, S.A. (1992) Anisotropy of Spatial Structures in the Middle Atmosphere. *Advances in Space Research*, **12**, 169-175. https://doi.org/10.1016/0273-1177(92)90462-7

[27] Sjoqvist, L. (2008) Laser Beam Propagation in Jet Engine Plume Environments: A Review. *Technologies for Optical Countermeasures V*, **7115**, 71150C. https://doi.org/10.1117/12.803543

[28] Hogge, C.B. and Visinsky, W.L. (1971) Laser Beam Probing of Jet Exhaust Turbulence. *Applied Optics*, **10**, 889-892. https://doi.org/10.1364/AO.10.000889

[29] Barrett, J.L. and Budni, P.A. (1992) Laser Beam Propagation through Strong Turbulence. *Journal of Applied Physics*, **71**, 1124-1127. https://doi.org/10.1063/1.351276

[30] Henriksson, M., Sjoqvist, L. and Gustafsson, O. (2006) Experimental Study of Mid-IR Laser Beam Wander Close to a Jet Engine Exhaust. *Proceedings of SPIE*, **6397**, 639709. https://doi.org/10.1117/12.689638

[31] Mahdieh, M.H. (2008) Numerical Approach to Laser Beam Propagation through Turbulent Atmosphere and Evaluation of Beam Quality Factor. *Optics Communications*, **281**, 3395-3402. https://doi.org/10.1016/j.optcom.2008.02.040

[32] Henriksson, M., Sjoqvist, L., Seiffer, D., Wendelstein, N. and Sucher, E. (2008) Laser Beam Propagation Experiments along and across a Jet Engine Plume. *Proceedings of SPIE*, **7115**, 71150E. https://doi.org/10.1117/12.799202

[33] Ding, C., Korotkova, O., Li, D., Zhao, D. and Pan, L. (2020) Propagation of Gaussian Schell-Model Beams through a Jet Engine Exhaust. *Optics Express*, **28**, 1037-1050. https://doi.org/10.1364/OE.381242

[34] Lutomirski, R.F. (1970) Propagation of a Finite Optical Beam in an Inhomogeneous Medium. *Applied Optics*, **10**, 1652-1658. https://doi.org/10.1364/AO.10.001652

[35] Bastiaans, M.J. (1978) The Wigner Distribution Function Applied to Optical Signals and Systems. *Optics Communications*, **25**, 26-30. https://doi.org/10.1016/0030-4018(78)90080-9